Talanta 221 (2021) 121600

Contents lists available at ScienceDirect

Talanta

journal homepage: www.elsevier.com/locate/talanta

Horseradish peroxidase-encapsulated DNA nanoflowers: An innovative signal-generation tag for colorimetric biosensor

Ruijin Zeng [a,c,1], Jun Wang [b,**,1], Qingshui Wang [a], Dianping Tang [c], Yao Lin [a,*]

[a] Central Laboratory at the Second Affiliated Hospital of Fujian Traditional Chinese Medical University, Collaborative Innovation Center for Rehabilitation Technology, Fujian University of Traditional Chinese Medicine, Fuzhou, Fujian, 350122, PR China
[b] Department of General Surgery at the Second Affiliated Hospital of Fujian Traditional Chinese Medical University, Collaborative Innovation Center for Rehabilitation Technology, Fujian University of Traditional Chinese Medicine, Fuzhou, Fujian, 350122, PR China
[c] Key Laboratory of Analytical Science for Food Safety and Biology (MOE & Fujian Province), Department of Chemistry, Fuzhou University, Fuzhou, 350108, PR China

ARTICLE INFO

Keywords:
Colorimetric biosensor
DNA nanoflowers
Rolling circle amplification
Enzyme encapsulation
DNA nanotechnology

ABSTRACT

Herein a versatile colorimetric biosensing platform was designed for sensitive, specific, and rapid screening of cancer-derived exosomes (HepG2 cell-derived) by introducing horseradish peroxidase -encapsulated DNA nanoflowers (HRP-DF) as the biorecognition elements and signal-generation tags. HRP was concurrently associated with the growing ultralong-chain DNA and the magnesium pyrophosphate crystals (Mg_2PPi) during the rolling circle amplification (RCA), thereby ultimately leading to the direct fixation of HRP in DFs. For demonstration, a linear DNA circular molecule encoding the complementary sequence of CD63 aptamer (a nucleic acid sequence that can highly bind to exosomes) was used as a starting amplification template to obtain HRP-DF with the high biorecognition ability of exosomes. Upon addition of target exosomes, a sandwiched reaction was carried out between the cholesterol-modified DNA probes-conjugated magnetic bead (MB) and the HRP-DFs, accompanying formation of ternary complexes (MB-exosomes-HRP-DF). After simple magnetic separation, the HRP carried on the ternary complexes (MB-exosomes-HRP-DF) initiated oxidation of 2,2′-azino-bis(3-ethylbenzothiazoline-6-sulphonic acid) (ABTS, nearly colorless) into green-colored oxidized ABTS in the presence of hydrogen peroxide (H_2O_2). The obvious color change (from nearly colorless to dark green) of ABTS-H_2O_2 system can be easily observed with the naked eye and accurately monitored by UV–visible spectrometry, which was also proportional to the concentration of exosomes. Impressively, HRP-DF-based biosensing platform exhibited satisfactory colorimetric responses toward target exosomes within the working range from 5.0×10^3 to 5.0×10^6 particles/μL at a low detection limit of 3.32×10^3 particles/μL. Combined with a one-step sandwich reaction, magnetic separation and HRP-DF-based color-changing, this system had the advantages of acceptable accuracy, strong anti-interference ability and good reproducibility.

1. Introduction

Advances in DNA nano/micro-scale construction technology through three-dimensional (3D) DNA editing and/or programmable self-assembly have enabled the creation of complex DNA superstructure with well-defined, sophisticated, and artificial shapes [1–3]. A highly prominent and fascinating feature of the 3D DNA superstructure and self-organized nanoassemblies framework lies in the fact that it can be versatile by positioning the components of common biological macromolecules (proteins, enzymes, medicine) on nano/micro-scale custom structure [4–6]. Recently, diverse protocols involving 3D DNA superstructure framework have been reported in the field of analytical nanoscience as well as diagnostic therapy because of excellent activities and operational biostability. Zeng et al. reported the coupling of double-enzyme-encapsulated DNA hydrogel with an enzyme-triggered photoelectrochemical bioetching reaction [7]. By conjugating two enzymes and biotin-modified long-chain dsDNA building blocks, the DNA-enzymes 3D network hydrogel was programmable self-assembly and one-step synthesized for glucose-driven sensing by using streptavidin as a cross-linker agent. Although DNA-enzymes 3D network

* Corresponding author.
** Corresponding author.
E-mail addresses: 1095077121@qq.com (J. Wang), yaolin@fjnu.edu.cn (Y. Lin).
[1] Ruijin Zeng and Jun Wang have contributed equally to this work.

https://doi.org/10.1016/j.talanta.2020.121600
Received 25 July 2020; Received in revised form 22 August 2020; Accepted 27 August 2020
Available online 2 September 2020

hydrogel synthesis method is simple and convenient with excellent activity, it cannot be a universal biosensor applicable because the encapsulation of specific enzyme is triggered by the corresponding substrate. Inspiringly, Kim et al. developed the method of protein-inorganic DNA nanoflowers by using mature rolling circle amplification (RCA) technology, which can efficiently load multiple proteins (BSA, RNase A, and cytochrome C as an example) while preserving the protein-activity of the payloads [6]. During the RCA process, the growing ultralong-chain ssDNA coexisting in the homogeneous reaction solution probably to mediate the nucleation-growth of high-concentration magnesium pyrophosphate (Mg_2PPi), thereby forming porous DNA-inorganic hybrid micro/nanostructures by anisotropic DNA liquid crystallization [8–10]. Interestingly, the ultralong-chain ssDNA with well-defined repeated units obtained by the RCA process is encoded with the corresponding aptamer in advance, and then the resulting DNA-inorganic nanoflower can play a versatile biorecognition function. Cheng et al. established a lateral flow biosensing system for the portable and sensitive smartphone-based photo-thermal quantitative detection of exosomes based on Au@Pd nano-popcorn with DNA flower [11]. The CD63 aptamer, a nucleic acid fragment with strong binding affinity and efficiency to the surface of exosomes, is encoded in the RCA amplification template and used as a biorecognition sequence for the synthesis of aptamer-functionalized DNA nanoflowers. Inspired by the above motivations, it was speculated that such self-assembled DNA-inorganic micro/nanostructures, programmed to contain target analyte aptamers with the enzyme, which may replace traditional recognition-amplification elements (enzyme-labeled antibodies and enzyme-labeled single-stranded nucleic acid), thus further improving specificity and sensitivity in a particularly feasible way.

Exosomes, a kind of membrane-bound extracellular phospholipid vesicle with a diameter of 30–150 nm, have been reported present in various bodily fluids. These nanovesicles carry enriched proteins and nucleic acids originated from parents' cells, including tetraspanin family (CD9, CD63 and CD81), adhesion molecules (integrins, lactadherin), heatshock proteins (Hsp 60, Hsp 70 and Hsp 90), messenger RNA and microRNA [11]. Accumulating evidence has revealed that exosomes become important mediators for regulating cell-to-cell communication by transferring biomolecules involving in both physiological and pathological processes [12]. Recently, more and more studies have been reported that exosomes may become an ideal non-invasive plasma biomarker for early-stage cancer diagnosis [13,14]. Consequently, accurate/reliable quantification, cost-effective and instant detection of exosomes level in complex biological fluids is of great significance and urgently desired in clinical diagnosis and treatment [15]. Toward this goal, herein we elaborately construct a high-performance and powerful colorimetric biosensor for the quantitative screening of exosomes by using horseradish peroxidase-encapsulated DNA flowers (HRP-DFs) with the biocatalytic color-changing system. In our sophisticated design, cholesterol-modified DNA probes-conjugated magnetic bead (MB) and CD63 aptamer-encoded HRP-DFs were employed as the biorecognition elements for target exosome, respectively. Similar to the traditional one-step sandwich immunoassay, when the target exosomes are present, the cholesterol-modified DNA probes-conjugated magnetic bead (MB) and CD63 aptamer-encoded HRP-DFs will bind to the surface of the exosomes to form a sandwich ternary complexes structure (MB-exosome-HRP-DFs). After magnetic separation, the resulting MB-exosome-HRP-DFs can catalyze the ABTS-H_2O_2 color-changing system. As a result, the detection of target exosomes is converted to the color change of the ABTS-H_2O_2 system, which is easily observed by the naked eye and accurately measured by ultraviolet–visible spectrometry (Scheme 1). This work not only provides an effective strategy for the synthesis of enzyme-encapsulated DFs with a well-defined structure but also sheds light on the development of powerful biorecognition elements and signal generation tags for traditional biosensors.

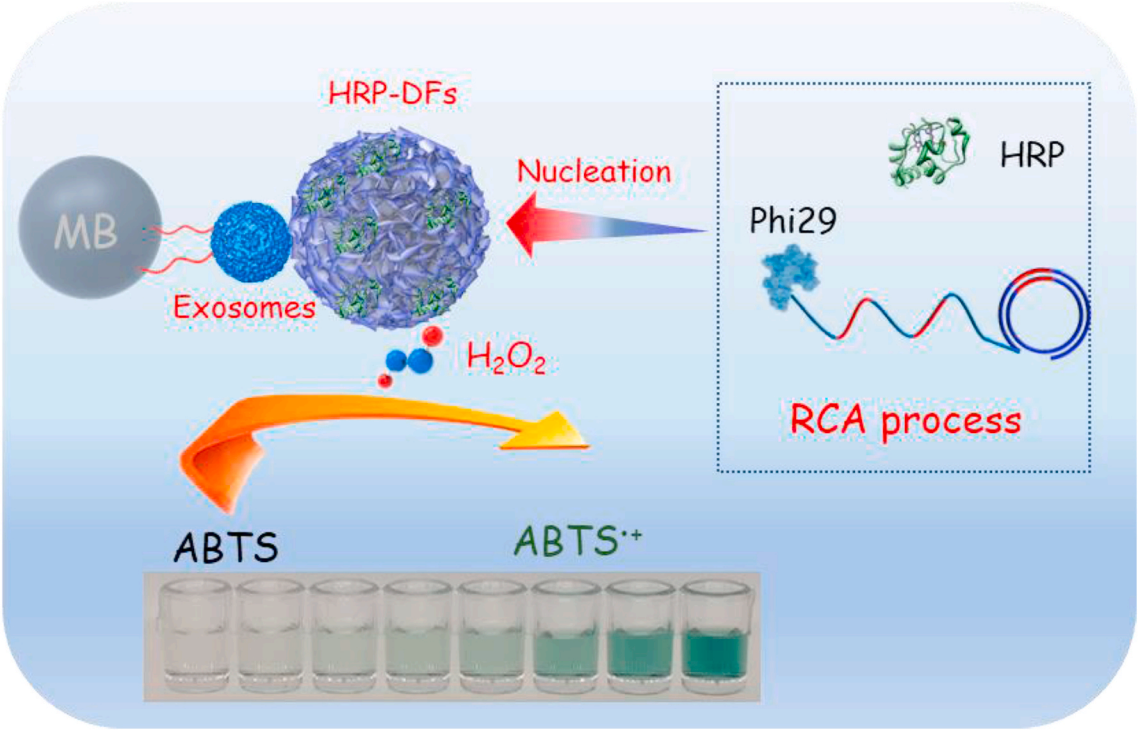

Scheme 1. Schematic illustration of colorimetric biosensor for the detection of target exosomes on cholesterol -modified DNA probes-conjugated magnetic bead (MB) and CD63 aptamer-encoded HRP-DF, based on catalyzing ABTS-H_2O_2 color-changing system (HRP-DF: horseradish peroxidase-encapsulated DNA nanoflowers; RCA: rolling circle amplification; phi 29: phi29 DNA polymerase).

2. Experimental

2.1. Reagent and material

2,2′-azino-bis(3-ethylbenzothiazoline)-6-sulfonate diammonium salt (ABTS; cat# A600002), T4 DNA ligase (cat# B600511), exonuclease I (Exo I; cat# C610019), horseradish peroxidase (HRP, ≥ 300 U/mg; cat# A600691), phi29 DNA polymerase (1.0 kU, cat# B300084), bovine serum albumin solution (BSA; 20 mg/mL), and deoxynucleotides (dNTPs; 10 mM, cat# B300576) were purchased from Sangon Biotech. Co., Ltd (Shanghai, China). Rhodamine B-labeled HRP and hepatocellular carcinoma cell line (HepG2)-derived exosomes were purchased from Xi'an Ruixi Biolog. Tech. Co. Ltd (Xi'an, China). Commercially ELISA kits including CEA, AFP and PSA) were purchased from Wuhan Cusabio Biotech. Co., Ltd (Wuhan, China). Streptavidin-modified Fe_3O_4 magnetic beads (MBs; 200 nm in diameter, cat# Mag9201-05) were purchased from Beijing Zhongkeleiming Daojin Tech. Co., Ltd (Beijing, China). All aqueous solutions in this experiment were prepared by using deionized water (18.2 MΩ cm^2). All HPLC-purified oligonucleotide sequences were purchased from Sangon Biotech. Co. Ltd (Shanghai, China). These sequences are listed as follows:

Capture probe: 5′-biotin-T_{40}-cholesterol-3'.

padlock probe: 5′-phosphate-AATATTATTCCAGCTGGCTAGCA TTAGTGTCACGGGAGCG.

AGGTGGGGTGGACTGCACCTTGAACGCTTATTATGATT-3'.

Primer DNA: 5′-AATAATATTAATCATAATA-3'.

2.2. Preparation of circular template DNA

Firstly, 5′-phosphorylated padlock probe (50 μM, 25 μL) and primer (50 μM, 45 μL) were co-hybridized in T4 DNA ligase buffer (10 μL of 10 × buffer; provided by the merchant package) by heating at 95 °C for 4 min, and then slowly cool to room temperature (RT) for 6 h. Subsequently, T4 DNA ligase (5 U/μL; 20 μL) was added, and the mixture solution was incubated at 20 °C for 12 h. The T4 DNA ligase in solution was completely inactivated by heating at 70 °C for 5 min. The circular template was acquired by treating with of Exo I (20 U/μL; 10 μL) in Exo I buffer (12 μL of 10 × buffer; provided by the merchant package) at 37 °C for 2 h to degrade the excess padlock probes and primers, followed by heating at 85 °C for 15 min to completely inactivate Exo I.

2.3. Synthesis of HRP-encapsulated DNA nanoflowers (HRP-DFs)

Circular template DNA (2.5 μM; 10 μL), dNTP (10 mM; 10 μL), HRP solution (50 μg/mL; 10 μL), phi29 DNA polymerase (10 U/μL; 5 μL) and deionized water (55 μL) are mixed in phi29 DNA polymerase buffer (10 μL of 10 × buffer, provided by the merchant package) at 25 °C for 30 h. The obtained white precipitate was washed with deionized water to remove any free HRP and unreacted DNA by centrifugation at 9500 g for 15 min [6,16]. The obtained HRP-DFs were redispersed in deionized water and kept at 4 °C refrigerator.

2.4. Colorimetric measurement toward target exosomes

Prior to colorimetric measurement, the biotinylated capture probes against target exosomes were initially conjugated to streptavidin-functionalized Fe_3O_4 magnetic beads (MBs; 200 nm in diameter) on the basis of typical biotin-avidin reaction [17,18]. In detail, biotinylated capture probes (100 μL, 10 μM) were first added into functionalMB solution (100 μL, 0.5 mg/mL), and then the mixture was incubated for 2 h at room temperature with gentle shaking on a shaker. Following that, the capture probe-conjugated MBs (capture-MB) were collected by using magnetic separation with an external magnet (note: The non-specifically absorbed capture probes on the magnetic beads were removed by washing with ultrapure water and purified with magnet).

Next, the as-prepared capture-MB was used for the detection of target exosomes with different concentrations with the assistance of HRP-DF as follows. Initially, exosome standards with various levels (0–5.0 × 10^6 particles/μL) were mixed with PBS buffer (200 μL, 10 mM, pH 7.4) containing 0.25% Tween-20, capture-MB (0.1 mg/mL) and HRP-DF (0.1 mg/mL). Thereafter, the mixture was incubated for 45 min at room temperature under slight shaking. The resultant bioconjugates (*i.e.*, MB-exosome-HRP-DF) were magnetically separated, and the collected samples were thrown into PBS (180 μL, 10 mM, pH 7.4). Following that, 20 μL of substrate solution including H_2O_2 (10 μL, 5 mM) and ABTS (10 μL, 40 mM) was injected into the above-prepared MB-exosome-HRP-DF solution. The mixture was shaken for 20 min as before for the color development. Meanwhile, the absorbance (a.u.) was measured from 380 nm to 500 nm on a UV-2700 spectrophotometer, and registered as the sensor signal relative to exosome concentration. All determinations were made at least in triplicate. All measurments were conducted at room temperature.

3. Results and discussion

3.1. Detailed characterization of DFs and HRP-DFs

In this work, the HRP-DF was used as a biorecognition element and signal-generation tag of the ABTS-H_2O_2 colorimetric sensing. For this reason, the successful synthesis of HRP-DFs with high biocatalytic activity and biorecognition ability is a key part of the whole sensor system. To clarify this point, native-polyacrylamide gel electrophoresis (PAGE, 12%, Fig. 1A) was used to verify whether DFs are self-assembled as high molecular weight products according to the envisaged RCA amplification pathway. It can be seen from lanes A and B that CD63 aptamer-encoded padlock probe shows a relatively low-mobility because it has a larger base number than the primer. After annealing the primer and padlock probe, then ligating with T4 DNA ligase and digesting with Exo I, an obvious band (lane C) with slightly lower mobility than the padlock probe appears. This clean and unique band corresponding to the generation of the circular template. Meanwhile, no extra bands corresponding to the position of the padlock probe and primers appeared, indicating the high efficiency of exonuclease digestion. After incubating the mixed solution of the circular template, dNTP, and phi29 DNA polymerase at 25 °C for 30 h, a high molecular weight band appeared at the opening of the lane D. The formation of high molecular weight DNA polymer illustrates the successful implementation of RCA. As a comparison, after adding HRP to the aforementioned DFs precursor, the RCA reaction was performed to obtain a high molecular weight DNA polymer (lane E) similar to lane D.

Further, the intrinsic microstructures, morphology, and particle size distribution of DFs and HRP-DFs were subjected to scanning electron microscopy (SEM; JEOLJSM-7001F, Japan), transmission electron microscopy (TEM; H-7700, Hitachi, Japan) and dynamic light scattering (DLS; Zetaszier Nano-ZS90, Malvern, UK). Evident from TEM image (Fig. 1B), the as-prepared DFs on the microgrid carbon support film exhibited flower-like superstructures with multi-layered sheets. Besides, the uniform morphology of DFs is approximately 962 nm with a narrow particle size distribution, which is in good agreement with the distribution results of dynamic light scattering (DLS, Fig. 1B, inset) (polymer dispersity index, PDI ~ 0.164). It can be clearly seen from the SEM image (Fig. 1C) that the 3D flower-like structure with a large number of smooth surfaces, which is also consistent with the TEM results. Next, the microstructure, morphology, and particle size distribution of HRP-DFs were also studied. From the TEM (Fig. 1D), DLS (Fig. 1D, inset), SEM (Fig. 1E) results obtained by HRP-DFs, there is no significant difference in the superstructure of the DNA polymer encapsulating the enzyme, which shows that the process of encapsulating the enzyme does not significantly affect the microstructure and morphology of the DFs. Corresponding elemental composition of the HRP-DFs was measured by energy dispersive spectroscopy (EDS) (Fig. 1F). Coexisting elements carbon (C, 25.89%), nitrogen (N, 5.04%), oxygen (O, 42.62%),

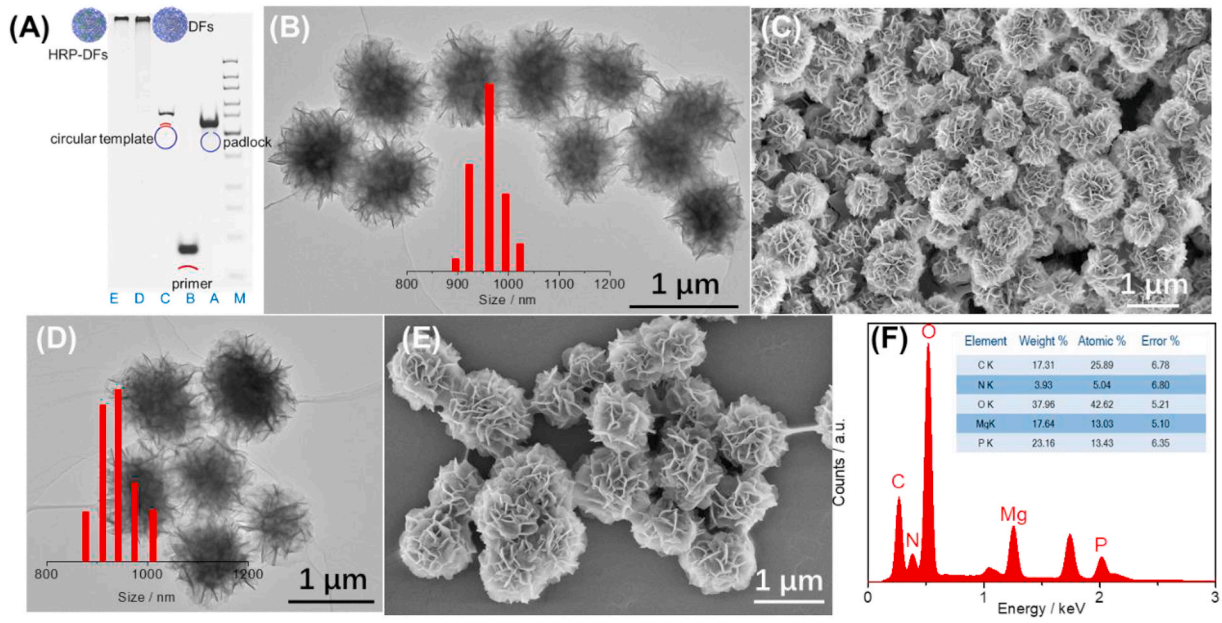

Fig. 1. (A) PAGE (12% gel) for different samples (lane M: 300 bp-marker; lanes A: padlock probe; lane B: primer; lane C: padlock probe + primer + T4 DNA ligase + Exo I; lane D: DFs (circular template + dNTP + phi29 DNA polymerase); lane E: HRP-DFs (circular template + dNTP + phi29 DNA polymerase + HRP)); (B) TEM image (inset: DLS analysis) and (C) SEM image of DFs; (D) TEM image (inset: DLS analysis) and (E) SEM image of HRP-DFs; (F) EDS element analysis recorded from the whole area of HRP-DFs.

magnesium (Mg, 13.03%), and phosphorus (P, 13.43%) mainly derived from the DNA superstructure framework and Mg_2PPi crystal in the HRP-DFs.

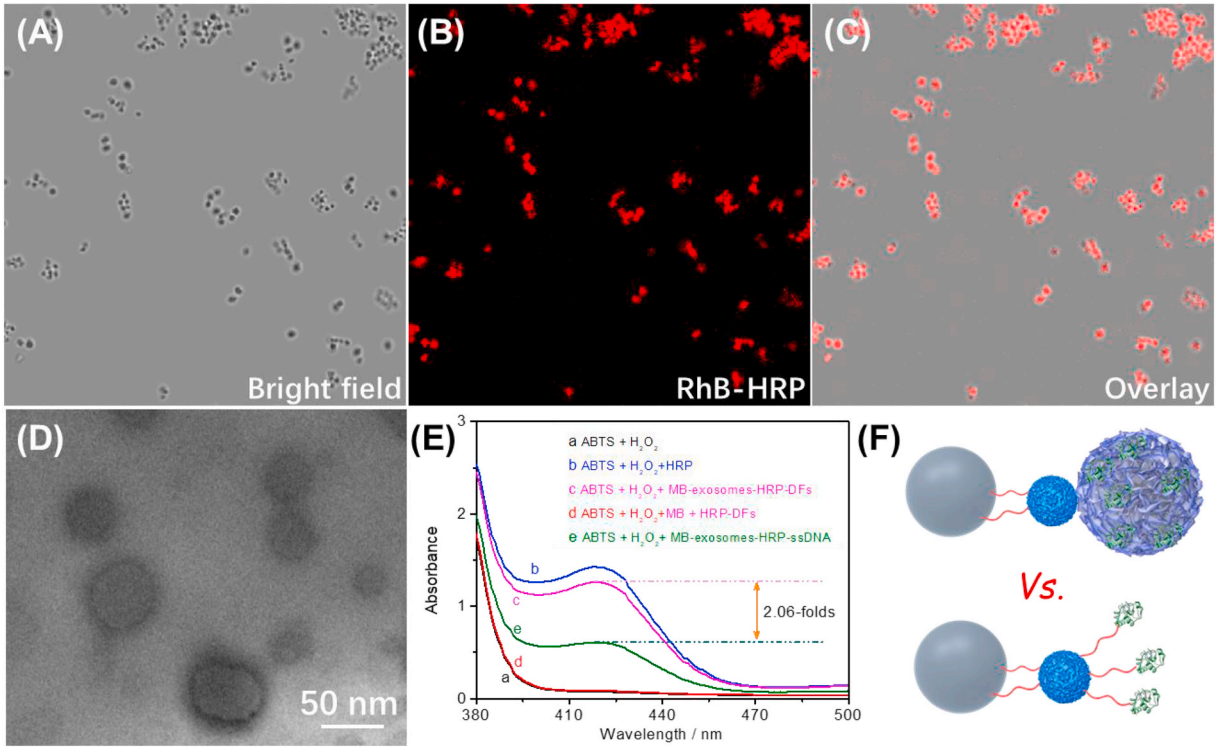

Fig. 2. (A–C) Confocal microscopy images of RhB (red fluorescence) labeled HRP-DFs (RhB-labeled HRP: 543 nm excitation wavelength); (D) TEM image of exosomes on carbon grid; (E) UV–vis absorption spectra of samples: (a) ABTS + H_2O_2, (b) ABTS + H_2O_2 + HRP, (c) ABTS + H_2O_2 + HRP + capture-MB + exosome + HRP-DF, (d) ABTS + H_2O_2 + HRP + capture-MB + HRP-DF, and (e) ABTS + H_2O_2 + HRP + capture-MB + exosome + HRP-ssDNA (note: The final concentrations of ABTS, H_2O_2, HRP, capture-MB, exosome and HRP-DFs were 2.0 mM, 0.25 mM, 5.0 μg/mL, 0.1 mg/mL, 5.0 × 10^6 particles/μL and 0.1 mg/mL, respectively); (F) Schematic diagram about the performance comparison of HRP-ssDNA and HRP-DFs. (For interpretation of the references to color in this figure legend, the reader is referred to the Web version of this article.)

3.2. Verification the feasibility of HRP-DFs-based ABTS-H_2O_2 color-changing system

To further verify HRP molecular is indeed encapsulated in DFs, RhB-labeled HRP is used as a fluorescent probe for positioning in a confocal laser scanning microscope. Under a given excitation wavelength, RhB-labeled HRP can emit strong red fluorescence in the field of laser scanning confocal microscope. In bright field view, HRP-DFs show black spots on low-magnification imaging (Fig. 2A). As expected, strong red fluorescence appears in the area corresponding to the bright field (Fig. 2B). The bright-field image and the fluorescence image are superimposed to obtain Fig. 2C to observe the location of RhB-labeled HRP in HRP-DFs [7]. Impressively, the position where the fluorescence appears coincides with the HRP-DFs in the bright field and there is no excess fluorescence in other positions. The above results clearly and powerfully illustrate that the HRP enzyme is encapsulated in DFs, and a reasonable centrifugation method can prevent the presence of HRP enzyme in the supernatant from affecting the performance of the sensing platform (high background signal and false positives).

Exosomes derived from HepG2 were used as model analytes to evaluate the performance of the HRP-DFs-based ABTS-H_2O_2 color-changing system. As TEM image is shown in Fig. 2D, the exosomes exhibit a typical cup-shaped membrane structure with a diameter ranging from 25 to 85 nm. Next, a series of comparative experiments under different conditions are studied to further verify the feasibility of the sensing system (Fig. 2E). From curve a, it can be shown that the single ABTS-H_2O_2 system cannot change the absorbance intensity of the entire homogeneous solution. When adding 5.0 μg/mL of HRP solution to the ABTS-H_2O_2 system, the absorbance intensity of the homogeneous solution increased significantly (curve b). Taking the exosomes concentration of 5×10^6 particles/μL as a model, MB-exosome-HRP-DFs obtained by sandwich reaction and magnetic separation were added to the ABTS-H_2O_2 system. As expected, the absorbance intensity increased significantly (curve *c vs*. curve *a*), indicating that the successful capture of exosomes and the enzyme encapsulated in HRP-DFs played an excellent catalytic effect. When the target exosomes are absent, the absorbance intensity of the solution is similar to that of the ABTS-H_2O_2 system alone (curve *d vs*. curve *a*). The above results show that the target exosomes are the root of signal changes. Besides, it also proved that there is almost no free HRP enzyme in the solution, which is consistent with the results of the laser scanning confocal microscope. These results indicated that the HRP-DFs-based ABTS-H_2O_2 biosensing system could be employed for the colorimetric detection of target exosomes.

To further elucidate the merits of HRP-DFs, HRP-labeled ssDNA encoding CD63 aptamer (HRP-ssDNA) was compared with HRP-DFs (Fig. 2F). Obviously, under the condition of the same exosomes concentration (5×10^6 particles/μL), the absorbance intensity of the HRP-DFs group (~1.2595 at 418 nm, curve '*b*') is 2.06 times that of the HRP-ssDNA group (~0.6079 at 418 nm, curve b). Moreover, the absorption absorbance of the HRP-DFs group could maintain 95.17, 93.22, 91.66, 90.77, 89.66 and 87.55% of the initial signal after storage for 1st, 2nd, 3rd, 4th, 5th and 6th week, respectively. For the HRP-ssDNA group, the absorbance intensity could maintain 90.34, 85.29, 81.64, 76.94, 71.66, and 70.36% of the initial signal after storage for 1st, 2nd, 3rd, 4th, 5th and 6th week, respectively. As previously reported, the reason why encapsulation of enzymes in DFs can greatly improve catalytic activity and maintain stability is likely to be a unique environment on inside DFs, especially the high charge density of DNA and metal ions (such as Mg^{2+}) to coordinate and stabilize enzyme molecules [19,20].

3.3. Optimization of experimental conditions

To acquire high sensitivity, factors influencing the analytical properties of HRP-DFs-based ABTS-H_2O_2 colorimetric assay should be optimized by using 5×10^6 particles/μL exosome as an example. Generally, the DNA framework and enzyme activity in HRP-DF may be affected by the pH value of the PBS detection solution. In this regard, we initially investigated the effect of PBS with different pH values (10 mM) on the analytical performance of the colorimetric assay. Obviously, a parabolic relationship between the pH value and absorbance was observed (Fig. 3A), with an initial increment followed by a decrement. A maximum absorbance was achieved at pH 7.4 PBS, which was chosen for the colorimetric measurement. Moreover, the colorimetric response of different incubation times was further studied. As shown in Fig. 3B, the steady-state absorbance value were achieved after 20 min. A longer incubation time did not cause the significant increase in the absorbance. To save the assay time and acquire an adequate signal, we selected 20 min as the incubation time in this work.

3.4. Dose responses of HRP-DF-based ABTS-H_2O_2 colorimetric toward target exosomes

By coupling with HRP-DFs-based biorecognition-signal amplification and ABTS-H_2O_2 strategy, the exosome standareds with different concentrations (0–5×10^6 particles/μL) were systematically detected. As the concentration of exosomes increased successively, the absorbance intensities increased monotonically, which resulted from the MB-exosomes-HRP-DFs-driven enzyme catalysis process of ABTS-H_2O_2 homogeneous system. A preferable linear-dependence absorbance intensity-exosomes concentration curves were obtained within the dynamic range (Fig. 4A) and the correlation equation could be described as y (absorbance intensities at 418 nm) = $0.3845 \times \log C_{[exosomes]} - 1.3592$ (particles/μL), ($R^2 = 0.9846$, $n = 7$) with maximum relative standard deviation RSD of 7.83% (Fig. 4B). The limit of detection (LOD) value of the colorimetric biosensor was assessed to be 3.32×10^3 particles/μL according to 3δ-formula (note: δ is the SD for 13-blank absorbance measurements), which was lower than available exosomes-strategies (Table 1).

The specificity of HRP-DF-based ABTS-H_2O_2 colorimetric biosensor was further systematically investigating with the intervention of several common human tumor biomarkers in serum, such as alpha-fetoprotein (AFP, 500 ng/mL), prostate-specific antigen (PSA, 500 ng/mL), and carcinoembryonic antigen (CEA, 500 ng/mL). As seen from Fig. 4C, these high-concentration of non-targets biomarkers only caused relatively low absorbance intensities in comparison with the background (PBS buffer), while the absorbance intensities of exosomes alone and mixtures containing exosomes increased significantly, revealing the satisfactory discrimination capability. Such excellent recognition ability is mainly ascribed to the cholesterol modified on the surface of the MB and the CD63 aptamer encoded in HRP-DFs, which has a strong affinity and binding ability on the surface of exosomes.

3.5. Detection of exosomes from clinical samples

To demonstrate the possibility of applying HRP-DF-based ABTS-H_2O_2 colorimetric biosensor for practical applications, we performed exosome concentration analysis by detecting four freshly collected clinical serum samples from two healthy donors and two cancer patients. Before the test, the ExoQuick kit was used to extract exosomes from the serum samples and then quantified by using the calibration equation shown in Fig. 4B. To evaluate the accuracy of our method, the concentration of exosomes (after extraction) was also quantified by nanoparticle tracking analysis (NTA). Notably, the concentration of exosomes from healthy individuals is significantly lower than in cancer patients (Fig. 5). Besides, the comparison results show that the concentration of exosomes measured by our method is equivalent to that obtained by NTA, which indicates that the accuracy of the relatively high accuracy of our proposed method for non-invasive detection of exosomes.

4. Conclusions

To sum up, this contribution describes a facile and versatile ABTS-

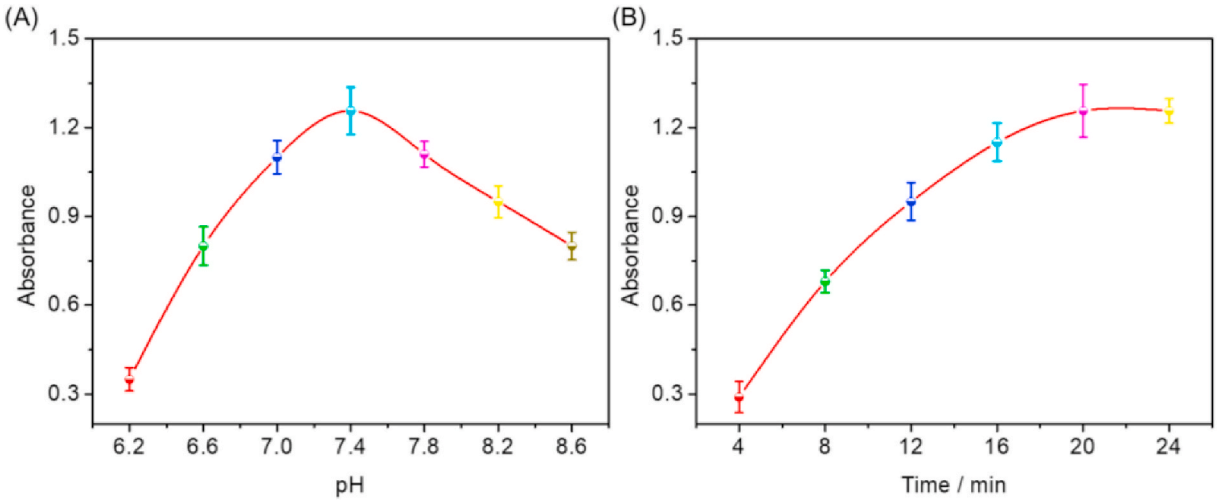

Fig. 3. Influence of (A) pH of PBS, (B) response time on the absorbance (a.u.) of HRP-DF-based ABTS-H_2O_2 colorimetric assay strategy (note: The error bars stand for the 95% confidence interval of the mean for absorbance responses).

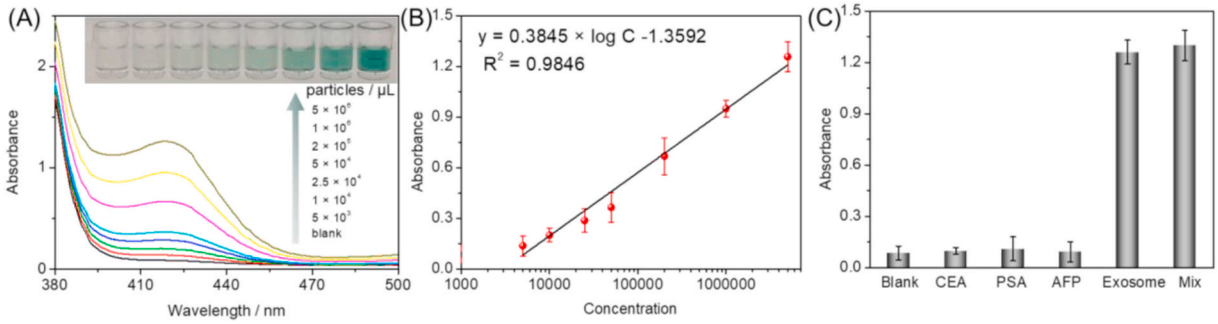

Fig. 4. (A) Absorbance (a.u.) of HRP-DF-based ABTS-H_2O_2 colorimetric assay toward exosome standards (0, 5×10^3, 1×10^4, 2.5×10^4, 5×10^4, 2×10^5, 1×10^6, and 5×10^6 particles/μL) (inset: The corresponding photographs); (B) calibration plots of absorbance peak (absorbance intensities at 418 nm) versus the decimal logarithm of the exosome-level (particles/μL); (C) the anti-interference ability against exosome (5×10^6 particles/μL) and three possible co-existence human biomarkers in serum, including CEA (500 ng/mL), PSA (500 ng/mL), AFP (500 ng/mL) (note: The aforementioned four analytes are included in the mixture).

Table 1
Comparison of different exosome detection schemes on analytical properties.

Transduced signal	Dynamic range (particles/μL)	LOD (particles/μL)	Ref.
Copper-mediated fluorescent biosensor	7.5×10^4–1.5×10^7	4.8×10^4	[21]
Lateral flow test strip with photothermal biosensor	1.0×10^5–1.0×10^7	1.4×10^4	[11]
DNA-capped-SWCNTs-based colorimetric aptasensor	1.84×10^6–2.21×10^7	5.2×10^5	[22]
Smartphone-enabled optofluidic platform	1.0×10^4–1.0×10^8	1.0×10^4	[23]
DNase I enzyme-aided fluorescence aptasensor	3.0×10^3–6.0×10^5	2.1×10^4	[24]
Screen-printed electrode-based biosensor	2.35×10^6–1.5×10^8	4.7×10^5	[25]
HRP-DFs-based ABTS-H_2O_2 colorimetric biosensor	5.0×10^3–5.0×10^6	3.32×10^3	This work

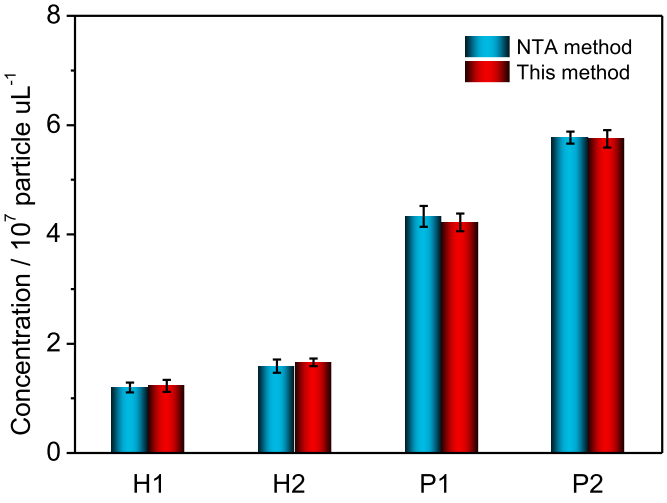

Fig. 5. Comparison of our method with ExoQuick kit-coupled NTA method for the determination of exosomes in serum samples from two healthy individuals (H) and two cancer patients (P).

H_2O_2 colorimetric biosensor for the rapid determination of cancer-derived exosomes (HepG2 cell-derived) by using horseradish peroxidase-encapsulated DNA flowers (HRP-DFs). Compared with traditional colorimetric sensors and exosomes analysis methods, this work creatively proposes to enzymes-encapsulate aptamers-encoded DNA flowers to serve as dual-function of biorecognition elements and signal-generating tags. Experimental results show that the enzyme-encapsulated DNA flower-like superstructure has better catalytic performance and biological stability than enzyme-labeled ssDNA. We hope that the "enzyme-encapsulation DNA superstructure" strategy can be used as universal biorecognition elements and signal-generating tags

to be further applied to various types of biosensors and analytes to form ternary complexes (nucleic acid-analyte-enzyme-encapsulation DFs or antibody-analyte-enzyme-encapsulation DFs) by encoding the corresponding aptamer sequence.

Credit author statement

Ruijin Zeng: Investigation, Roles/Writing-original draft. Jun Wang: Methodology; Data curation; Qingshui Wang: Conceptualization; Dianping Tang: Methodology; Resources; Supervision; Yao Lin: Resources; Supervision.

Declaration of competing interest

The authors declare that they have no known competing financial interests or personal relationships that could have appeared to influence the work reported in this paper.

Acknowledgments

The authors acknowledge financial support from the National Natural Science Foundation of China (21675029 & 21874022), and Health-Education Joint Research Project of Fujian Province (WKJ2016-2-15).

References

[1] F. Praetorius, B. Kick, K. Behler, M. Honemann, D. Weuster-Botz, H. Dietz, Biotechnological mass production of DNA origami, Nature 552 (2017) 84–87.
[2] M. Jones, N. Seeman, C. Mirkin, Programmable materials and the nature of the DNA bond, Science 347 (2015) 1260901.
[3] P. Wang, T. Meyer, V. Pan, P. Dutta, Y. Ke, The beauty and utility of DNA origami, Inside Chem. 2 (2017) 359–382.
[4] S. Douglas, I. Bachelet, G. Church, A logic-gated nanorobot for targeted transport of molecular payloads, Science 335 (2012) 831–834.
[5] K. Bujold, J. Hsu, H. Sleiman, Optimized DNA "nanosuitcases" for encapsulation and conditional release of siRNA, J. Am. Chem. Soc. 138 (2016) 14030–14038.
[6] E. Kim, L. Zwi-Dantsis, N. Reznikov, C. Hansel, S. Agarwal, M. Stevens, One-pot synthesis of multiple protein-encapsulated DNA flowers and their application in intracellular protein delivery, Adv. Mater. 29 (2017) 1701086.
[7] R. Zeng, Z. Huang, Y. Wang, D. Tang, Enzyme-encapsulated DNA hydrogel for highly effcient electrochemical sensing glucose, ChemElectroChem 7 (2020) 1537–1541.
[8] E. Kim, S. Agarwal, N. Kim, F. Hage, V. Leonardo, A. Gelmi, M. Stevens, Bioinspired fabrication of DNA-inorganic hybrid composites using synthetic DNA, ACS Nano 13 (2019) 2888–2900.
[9] R. Hu, X. Zhang, Z. Zhao, G. Zhu, T. Chen, T. Fu, W. Tan, DNA nanoflowers for multiplexed cellular imaging and traceable targeted drug delivery, Angew. Chem. Int. Ed. 53 (2014) 5821–5826.
[10] J. Lee, J. Hong, D. Bonner, Z. Poon, P. Hammond, Self-assembled RNA interference microsponges for efficient siRNA delivery, Nat. Mater. 11 (2012) 316–322.
[11] N. Cheng, Y. Song, Q. Shi, D. Du, D. Liu, Y. Luo, W. Xu, Y. Lin, Au@Pd nanopopcorn and aptamer nanoflower assisted lateral flow strip for thermal detection of exosomes, Anal. Chem. 91 (2019) 13986–13993.
[12] S. Bellingham, B. Guo, B. Coleman, A. Hill, Exosomes: vehicles for the transfer of toxic proteins associated with neurodegenerative diseases? Front. Physiol. 3 (2012) 1–12.
[13] T. Whiteside, Tumor-derived exosomes and their role in cancer progression, Adv. Clin. Chem. 74 (2016) 103–141.
[14] Y. Soung, S. Ford, V. Zhang, J. Chung, Exosomes in cancer diagnostics, Cancers 9 (2017) 8–19.
[15] Y. Tanaka, H. Kamohara, K. Kinoshita, J. Kurashige, H. Baba, Clinical impact of serum exosomal microRNA-21 as a clinical biomarker in human esophageal squamous cell carcinoma, Cancer 119 (2013) 1159–1167.
[16] Y. Yan, J. Li, W. Li, Y. Wang, W. Song, S. Bi, DNA flower-encapsulated horseradish peroxidase with enhanced biocatalytic activity synthesized by an isothermal one-pot method based on rolling circle amplification, Nanoscale 10 (2018) 22456–22465.
[17] R. Zeng, Z. Luo, L. Zhang, D. Tang, Platinum nanozyme-catalyzed gas generation for pressure-based bioassay using polyaniline nanowires-functionalized graphene oxide framework, Anal. Chem. 90 (2018) 12299–12306.
[18] R. Zeng, J. Tao, D. Tang, D. Knopp, J. Shu, X. Cao, Biometric-based tactile chemomechanical transduction: an adaptable strategy for portable bioassay, Nanomater. Energy 71 (2020) 104580.
[19] Y. Wang, E. Kim, Y. Lin, N. Kim, W. Kit-Anan, S. Gopal, S. Agarwal, P. Howes, M. Stevens, Rolling circle transcription-amplified hierarchically structured organic-inorganic hybrid RNA flowers for enzyme immobilization, ACS Appl. Mater. Interfaces 11 (2019) 22932–22940.
[20] R. Zeng, W. Wang, G. Cai, Z. Huang, J. Tao, D. Tang, C. Zhu, Single-atom platinum nanocatalyst-improved catalytic efficiency with enzyme-DNA supermolecular architectures, Nanomater. Energy 74 (2020) 104931.
[21] F. He, J. Wang, B. Yin, B. Ye, Quantification of exosome based on a copper-mediated signal amplification strategy, Anal. Chem. 90 (2018) 8072–8079.
[22] Y. Xia, M. Liu, L. Wang, A. Yan, W. He, M. Chen, J. Lan, J. Xu, L. Guan, J. Chen, A visible and colorimetric aptasensor based on DNA-capped single-walled carbon nanotubes for detection of exosomes, Biosens. Bioelectron. 92 (2017) 8–15.
[23] J. Ko, M. Hemphill, D. Gabrieli, L. Wu, V. Yelleswarapu, G. Lawrence, W. Pennycooke, A. Singh, D. Meaney, D. Issadore, Smartphone-enabled optofluidic exosome diagnostic for concussion recovery, Sci. Rep. 6 (2016) 31215.
[24] H. Wang, H. Chen, Z. Huang, T. Li, A. Deng, J. Kong, DNase I enzyme-aided fluorescence signal amplification based on graphene oxide-DNA aptamer interactions for colorectal cancer exosome detection, Talanta 184 (2018) 219–226.
[25] S. Yadav, K. Boriachek, M. Islam, R. Lobb, A. Moller, M. Hill, M. Hossaine, N. Nguyen, M. Shiddiky, An electrochemical method for the detection of disease-specific exosomes, ChemElectroChem 4 (2017) 967–971.